



OPEN

## Mechanistic insights into photochromic 3*H*-naphthopyran showing strong photocoloration

Błażej Gierczyk<sup>1</sup>, Michał F. Rode<sup>2</sup>✉ & Gotard Burdzinski<sup>3</sup>✉

3,3-Diphenylbenzo[*f*]chromene (**1**) represents an important architectural platform for photochromic systems. Since the practical utility of such chromophores is largely dependent upon the kinetics of coloration and decoloration, elucidating the mechanistic details of these processes is of great value. Toward this end, we studied the photochromic reaction of (3-(2-methoxyphenyl)-3-phenyl-3*H*-benzo[*f*]chromene (**2**) by both time-resolved UV–vis and mid-IR spectroscopies. We found that irradiation of **2** at 365 nm generates long-lived colored *transoid-cis* isomers with lifetimes of 17.1 s and 17.5 min (at 21 °C) and even longer-lived *transoid-trans* isomers with a lifetime of 16 h. These experimental results were supplemented with *ab initio* ground-state and excited-state calculations, and the resulting theoretical interpretation may be useful for the design of new photochromic systems with optimized photofunctionality.

Among the known photochromic compounds, the family of 3,3-diphenyl-3*H*-naphtho[2,1-*b*]pyrans (**1**) has attracted great interest in the field of ophthalmic lens production<sup>1–4</sup>. Compound **1**, exhibiting both P and T type photochromism, has been the subject of fundamental research<sup>5–13</sup>. In the photochromic reaction under typical conditions two colored species are formed (Fig. 1): *transoid-cis* TC (which fades rapidly) and *transoid-trans* TT (which fades more slowly)<sup>5</sup>. Synthetic changes in the structural pattern of **1** can tune its properties to fulfil the requirements of a particular application.

When the application requires a relatively fast decoloration rate, the presence of the long-lived TT form is unwanted. Efforts are focused then on designing derivatives of **1** with a minimized TT contribution in the photoreaction. Under typical experimental conditions with UV irradiation, the active channel for TT generation is TC → TT photoisomerization, which is a *single-twist* long amplitude motion<sup>11,13</sup> occurring in the excited state (*S*<sub>1</sub>). Strong competition of the other TC excited state deactivation channels can minimize the TC → TT photoisomerization yield. For example, if the potential-energy landscape of the initially photoexcited TC *S*<sub>1</sub> state favors a *bicycle-pedal* motion, the isomerization path might be quickly aborted through *S*<sub>1</sub> → *S*<sub>0</sub> internal conversion populating the form with the geometry close to that of the starting TC form<sup>12,13</sup>. Such a deactivation path can reduce the TC → TT photoisomerization yield, as reported for derivative of **1** with a methoxy group inserted at the position 10<sup>13,14</sup>.

The thermal fading rate of colored TC and TT isomers is also a key parameter of photochromic materials based on derivatives of **1**. Appropriate substituents in the skeleton of **1** can be used to tune the TC color fading rate which depends on the ground state potential energy landscape<sup>15</sup>. A key role in this process is played by the *cisoid-cis* intermediate form (INT) lying midway between the colored TC form (see Fig. 2), and the colorless CF form<sup>15</sup>. The relationship between the energy barriers  $\Delta E^{\text{INT-TC}}$  and  $\Delta E^{\text{INT-CF}}$  separating the intermediate INT from nearby global and local minima may either decelerate the INT → CF process (favoring the return to the colored TC form) or accelerate the process (favoring the ring-closing reaction). For instance, the  $\Delta E^{\text{INT-TC}}$  barrier for **1** is lower than  $\Delta E^{\text{INT-CF}}$  (Fig. 2), which makes the apparent TC lifetime relatively long (9.3 s at 21 °C in cyclohexane).

The opposite situation ( $\Delta E^{\text{INT-TC}} > \Delta E^{\text{INT-CF}}$ ) has been reported for 3*H*-naphthopyrans with phenyl substitution at position 2<sup>15</sup>. The apparent TC lifetime is remarkably short (only 30 μs) in solution at room temperature<sup>16</sup>. On the other hand, one can expect that a slow decoloration would help to achieve a strong photocoloration

<sup>1</sup>Faculty of Chemistry, Adam Mickiewicz University in Poznań, Uniwersytetu Poznańskiego 8, 61-614 Poznań, Poland. <sup>2</sup>Institute of Physics, Polish Academy of Sciences, Aleja Lotników 32/46, 02-668 Warsaw, Poland. <sup>3</sup>Faculty of Physics, Adam Mickiewicz University in Poznań, Uniwersytetu Poznańskiego 2, 61-614 Poznań, Poland. ✉email: mrode@ifpan.edu.pl; gotardb@amu.edu.pl

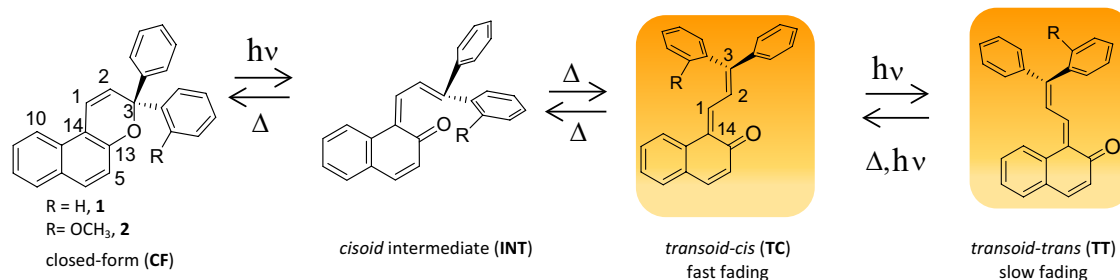


**Figure 1.** UV excitation of 3,3-diphenyl-3H-naphtho[2,1-b]pyran (**1**) converts the closed form CF to color isomers TC (short-lived) and TT (long-lived), with the intermediacy of *cisoid-cis* form INT (ultrashort-lived)<sup>11</sup>. Compound **2** with a methoxy group implemented at one of the phenyl rings at *ortho* position is selected for studies of a strong photochromation effect.

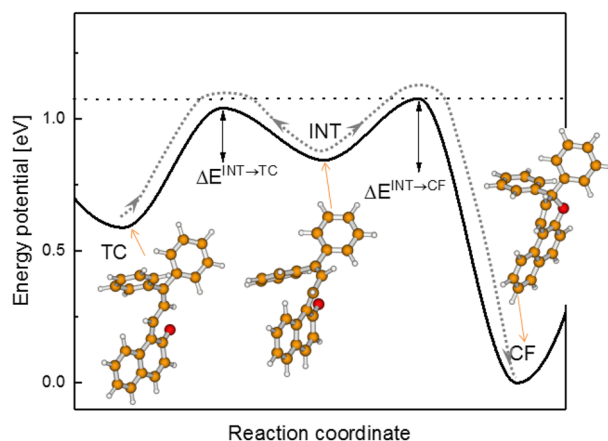


**Figure 2.** Thermal decoloration of TC → CF for compound **1** involves two reaction steps TC → INT and INT → CF, the first step is reversible<sup>15</sup>.

effect in the photostationary state. It is widely accepted that inclusion of a bulky substituent at the *ortho* position of one of the phenyl rings in **1** would result in a substantial extension of the thermal fading half-life  $\tau_{1/2}$ <sup>2,4,17–21</sup>. The half-life  $\tau_{1/2}$  of the open forms gets longer with increasing size of the *ortho* substituent (in the order of H → F → MeO → Me → Cl → Br → I) in the phenyl ring of 3-aryl-3-(4-pyrrolidinophenyl)naphtho[2,1-*b*]pyrans<sup>22</sup>. A remarkably slow-decoloration rate remains an intriguing feature for mechanistic and spectroscopic investigations.

For our studies we selected 3-(2-methoxyphenyl)-3-phenyl-3H-benzo[*f*]chromene (**2**), Fig. 1, as a candidate for a material with the strongest UV activated coloration. The relatively simple structure of **2** facilitates ab initio quantum-chemical calculations for the excited state, while the stages of the photochromic reaction can be studied in detail with experimental techniques such as the time-resolved UV-vis and mid-IR spectroscopies.

## Experimental

**Materials.** Compound **1** was purchased from TCI. Compound **2** was synthesized following the procedures described in the Supplementary Information. In the time-resolved spectroscopic investigation cyclohexane of spectroscopic grade from Sigma Aldrich was used for solution preparation.

**Time-resolved UV-vis and mid-IR spectroscopies.** Changes in UV-vis absorption spectra and kinetics were recorded using three configurations.

- (1) Jasco V-550 spectrophotometer with a modified cell compartment. The solution in 1 cm × 1 cm fused silica cuvette was placed into a temperature-controlled cuvette holder (Flash 300, Quantum Northwest) with stirring switched on. UV LED ( $\lambda_{\text{exc}} = 365$  nm, Thorlabs M365LP1) was used to induce the photochromic reaction (as in the two other configurations below).
- (2) Similar arrangement with a temperature-controlled cuvette holder and white light generated by a xenon lamp (Applied Photophysics), equipped with a bundle fiber, as a probing beam. The probing beam was passed through an almost-closed iris to ensure low white light intensity. The UV-vis spectra were recorded by an Ocean Optics FLAME-T-VIS-NIR-ES USB spectrometer at the sampling rate of 10 spectra per second.

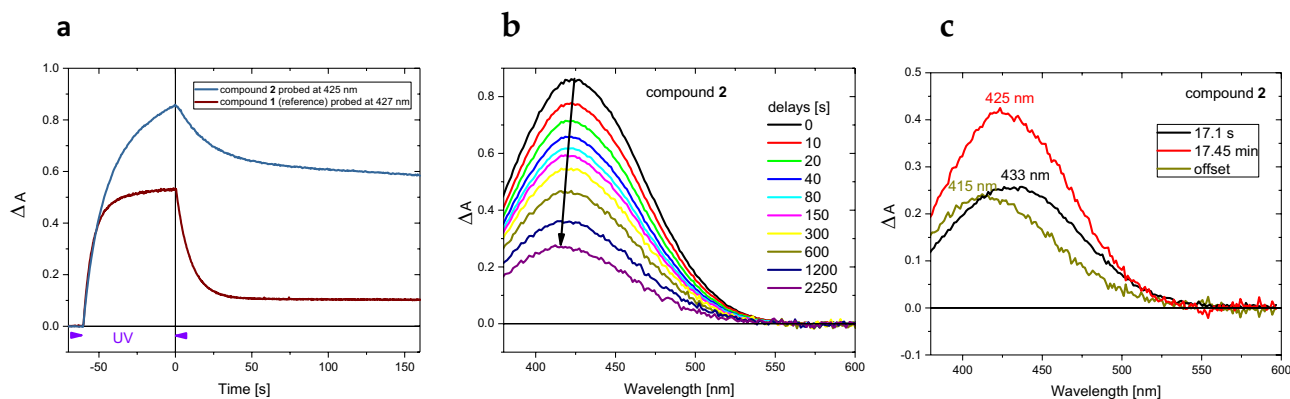


**Figure 3.** (a) Kinetics of the changes in absorption as a result of UV irradiation ( $4.1 \text{ mW/cm}^2$ ) in the period of 60 s for **2** and the reference **1** in cyclohexane at  $21 \text{ }^\circ\text{C}$  (both solutions prepared with the same absorbance  $A(365 \text{ nm}, 1 \text{ cm})=0.24$ ). (b) Transient UV-vis absorption spectra for **2** after switching off UV irradiation. (c) Decay associated spectra of the TC (17.1 s and 17.5 min) and TT isomers (the offset, long-lived population) obtained by global analysis using a biexponential function.

- (3) Acquisition mid-IR spectra upon simultaneous measurements in UV-vis spectral range has been described recently<sup>11</sup>. A Bruker Tensor 27 FT-IR spectrometer was equipped with an MCT detector, with a spectral resolution of  $4 \text{ cm}^{-1}$  and a sampling rate of  $1.15 \text{ s}^{-1}$ . The UV-vis probing light was generated from the xenon lamp. An Ocean Optics spectrophotometer was used for recording of UV-vis spectra. A Harrick Scientific cell was used with 2 mm thick  $\text{CaF}_2$  window and a 0.63 mm spacer.

**Theoretical calculations.** The equilibrium geometries of the CF conformers and their isomers in the closed-shell ground state ( $S_0$ ) were obtained with the MP2 method<sup>23</sup> with no imposed symmetry constrains. The energy of the most stable form  $\text{CF}_c$  (Table S1, Supplementary Information) was assumed as the reference energy for higher energy structures. The excited-state ( $S_1$ ) equilibrium geometries were determined with the second-order algebraic diagrammatic construction ADC(2) method<sup>24–26</sup>. The correlation-consistent valence double zeta basis set with polarization functions on all atoms (cc-pVDZ)<sup>27</sup> was used in these calculations as well as in the potential energy profiles and surfaces. The vertical excitation energies and response properties of the lowest singlet excited states were calculated using the CC2 methods<sup>28,29</sup>. The basis set augmented with the diffuse functions aug-cc-pVDZ was also used to compute vertical excitation energies of the molecular system. All calculations were performed using the TURBOMOLE program package<sup>30</sup>.

## Results and discussion

The stationary UV-vis absorption spectrum of **2** in cyclohexane (Figure S1, Supplementary Information) is similar to that of the reference compound **1**<sup>11</sup>, reflecting structural similarities between the two derivatives. In the structure of **1**, each phenyl ring has two *ortho* positions that can be substituted by a methoxy group, thus, four respective conformers of **2** are taken into account in the calculations. These conformers of the CF form are in thermal equilibrium in freshly prepared solution (indicated with subscripts: a, b, c, and d, see Table S1). The selection of wavelength at 365 nm induces the electronic transition  $S_0 \rightarrow S_1(\pi, \pi^*)$  separately in each CF form, which opens up along the  $\text{C}_3\text{-O}_4$  photodissociation pathway, as in **1**<sup>11</sup>. The photoinduced pyran ring-opening process can lead to the colored-isomers CTC and TTC. All the CF, TC and TT conformers potentially involved in the photoreaction, along with their calculated vertical excitation energies ( $\Delta E^{\text{VE}}$ ) simulating UV-vis absorption spectra, are collected in Table S1. The strong  $S_0 \rightarrow S_2(\pi, \pi^*)$  transitions for colored TC forms are slightly redshifted vs. those of TT forms; a similar trend was observed for the parent compound **1**<sup>11</sup>.

To study the photochromic reaction by changes in UV-vis absorption spectra, a UV LED light at 365 nm was used for sample excitation, while a xenon lamp was used for probing. Figure 3a shows the kinetics probed at 425 nm upon 60-s exposure a solution of **2** in cyclohexane to UV light.

Compared to **1**, compound **2** produces a stronger absorption signal upon UV irradiation (Fig. 3a), and after cessation of UV irradiation its color fading occurs at a lower rate. The quantum yield of TC formation is similar for **2** and **1** (0.745<sup>11</sup>), since the early signal rise in the  $-55$  to  $-60$  s time window shows the same slope and the TC molar extinction coefficients are comparable (see Supplementary Information). Figure 3b shows the evolution of the transient UV-vis absorption spectra in the time window of 0–2250 s. Global analysis of data (Fig. 3c) reveals three distinct populations: TC1 with the absorption band peaking at 433 nm and a lifetime of 17.1 s, TC2 with the band maximum at 425 nm and a 17.5 min lifetime, and TT with a maximum at 415 nm and a long lifetime. The TT lifetime of 16 h was determined in an additional experiment performed in the time window of 40 h (Figure S2). The respective molar extinction coefficients,  $\epsilon_{\text{max}}(\text{TC1}) \approx 18,900 \text{ M}^{-1} \text{ cm}^{-1}$ ,  $\epsilon_{\text{max}}(\text{TC2}) \approx 18,700 \text{ M}^{-1} \text{ cm}^{-1}$  and  $\epsilon_{\text{max}}(\text{TT}) \approx 29,500 \text{ M}^{-1} \text{ cm}^{-1}$ , are deduced from the simultaneously recorded changes in the UV-vis and mid-IR spectral ranges (see Figure S3, Supplementary Information). Thus, one can estimate from the data shown in Fig. 3 that at the moment of UV irradiation cessation, the conversion of CF population to colored forms is 69% and the concentrations of [TC1], [TC2] and [TT] are:  $1.4 \times 10^{-5} \text{ M}$ ,  $2.2 \times 10^{-5} \text{ M}$  and  $0.8 \times 10^{-5} \text{ M}$ , respectively. In addition, the FT-IR spectroscopy provides a confirmation of our signal assignment to TC and

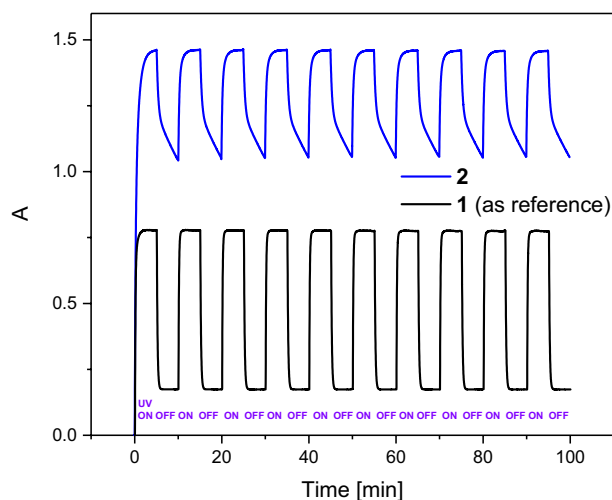


**Figure 4.** Kinetics of absorption upon switching on and off UV light at 365 nm ( $4.1 \text{ mW/cm}^2$ ) for **2** and **1** in cyclohexane probed at 430 nm using a Jasco spectrophotometer, temperature set at  $21^\circ\text{C}$ . Solutions prepared with the same absorbance  $A(365 \text{ nm}, 1 \text{ cm}) = 0.39$ .

TT isomers, since the C=O stretching absorption band of TC is located at a lower frequency than that of TT, as has been already observed for the reference compound **1** (TC at  $1644 \text{ cm}^{-1}$  and TT at  $1655 \text{ cm}^{-1}$ ).

Photocycle reproducibility observed for **2** in cyclohexane is similar to that for **1**, which is known to have high fatigue resistance (Fig. 4).

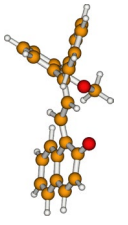
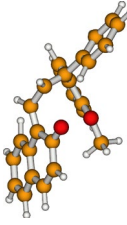
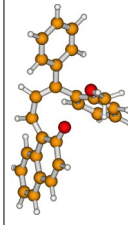
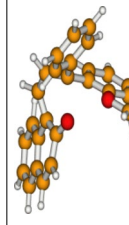
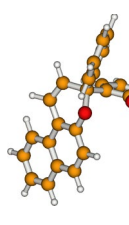
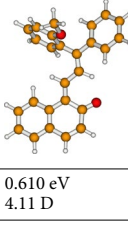
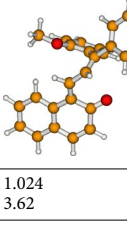
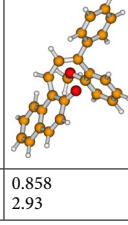
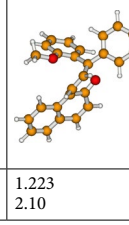
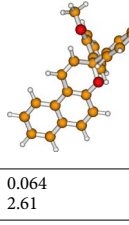
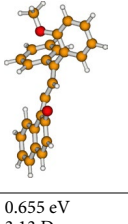
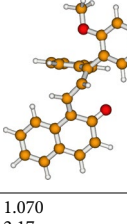
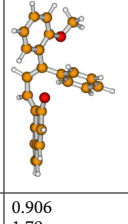
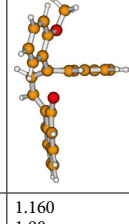
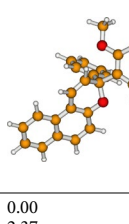
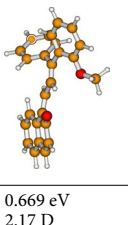
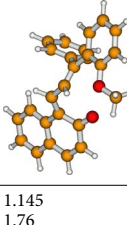
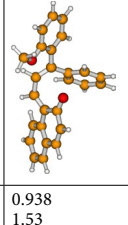
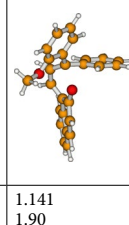
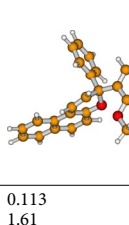
**Why do TC forms differ in decoloration kinetics?** The TC form in 3*H*-naphthopyrans is photogenerated in a single-photon absorption process<sup>11</sup>. A single TC isomer is generated from compound **1**, while four TC isomers from compound **2** should be taken into consideration. The geometries of these conformers are presented in the first column in Table S1. CTC<sub>a</sub> and CTC<sub>b</sub> are energetically more stable than TTC<sub>c</sub> and TTC<sub>d</sub>. Each of the four TC isomers is a colored species which, under thermal conditions, fades towards the respective closed CF form via a single *cisoid-cis* intermediate INT geometry located on the ground-state potential energy pathway. Each of the four S<sub>0</sub>-state pathways is characterized by a slightly different energy barriers separating the intermediate INT structure from the local TC and CF minima, which influence the apparent fading rate of each TC isomer. Energy barriers are shown in Table 1.

The first reaction step in the TC fading process is TC → INT isomerization, which must overcome a relatively high energy barrier  $\Delta E^{\text{TC-OUT}}$  ( $\sim 0.38\text{--}0.48 \text{ eV}$ ), to reach a highly energetic *cisoid-cis* INT intermediate in an endothermic process. In the second step, this intermediate can follow (1) an exothermic reaction towards the final closed-pyran ring CF form or (2) an alternative reverse process towards the TC form (Figure S4, Supplementary Information). As one can see in Table 1, the  $\Delta E^{\text{INT-CF}}$  barrier towards the final CF for each fading pathway is usually higher than the respective  $\Delta E^{\text{INT-TC}}$  barrier towards the initial TC form (except for the TTC<sub>d</sub> pathway, for which the TS<sub>2d</sub> structure ( $E^a = 1.145 \text{ eV}$ ) is slightly more destabilized due to O...O repulsion). Such a situation ( $\Delta E^{\text{INT-CF}} > \Delta E^{\text{INT-TC}}$ ) favors deceleration of the TC fading process, since once INT is formed it would rather repopulate the TC form. This may explain long TC lifetimes observed in the experiment for **2** (17.1 s and 17.5 min) in comparison to that of **1** (9.3 s,  $\Delta E^{\text{INT-CF}} = 0.233 \text{ eV}$  and  $\Delta E^{\text{INT-TC}} = 0.196 \text{ eV}$ <sup>13,15</sup>).

In order to assign each of the two TC lifetimes (17.1 s and 17.5 min) to the respective CTC and TTC families, we should consider their depopulation following the S<sub>0</sub>-state energetic profile (Figure S4). While the  $\Delta E^{\text{INT-TC}}$  barrier of  $\sim +0.16 \text{ eV}$  is the same for all the considered TC isomers (except for TTC<sub>d</sub>), it is the  $\Delta E^{\text{INT-CF}}$  barrier that seems to be critical. Since  $\Delta E^{\text{INT-CF}}$  is higher for CTC than for TTC ( $\sim +0.35$  vs.  $0.25 \text{ eV}$ ), the equilibrium of CTC<sub>a</sub> and CTC<sub>b</sub> is responsible for the long 17.5 min time-constant. The short time-constant (17.1 s) should be then ascribed to the TTC forms (equilibrium of TTC<sub>c</sub> and TTC<sub>d</sub>). The respective equilibria (CTC<sub>a</sub> – CTC<sub>b</sub> and TTC<sub>c</sub> – TTC<sub>d</sub>) are confirmed by the relatively low interconversion S<sub>0</sub>-state energy barriers of  $\sim +0.2 \text{ eV}$ .

To support the idea that the high value of the  $\Delta E^{\text{INT-CF}}$  barrier is a decisive parameter in longer fading time of CTC forms, we analyzed the geometries of the transition state TS1 structures. Indeed, the presence of a methoxy group is the cause of the O...O repulsion in TS1<sub>a</sub> ( $E^a = 1.185 \text{ eV}$ , see Table 1) or 10*H*...OCH<sub>3</sub> steric hindrance in TS1<sub>b</sub> ( $E^a = 1.223 \text{ eV}$ ). The *ortho*-methoxy substituent increases the electron density on that aromatic ring, which has a stabilizing effect on the *cisoid-cis* INT geometry through increased  $\pi$ -stacking of the aryl and naphthalenone moieties. This is responsible for a higher  $\Delta E^{\text{INT-CF}}$  barrier in the case of INT<sub>a</sub> and INT<sub>b</sub> ( $+0.341 \text{ eV}$  and  $+0.364 \text{ eV}$ ) vs. INT<sub>c</sub> and INT<sub>d</sub> ( $+0.254 \text{ eV}$  and  $+0.203 \text{ eV}$ ).

**Mechanism of the TC → TT photoisomerization reaction in the singlet excited state.** The act of photon absorption by each TC isomer activates the two double bonds present in the C<sub>14</sub>=C<sub>1</sub>–C<sub>2</sub>=C<sub>3</sub> bridge linking the naphthalenone skeleton with the diphenylmethylene rotor. This double bond activation allows free rotation about these bonds in the singlet excited state. As already shown for **1** derivatives<sup>13</sup>, this rotation can

Form	$\Delta E^{\text{TC-out}}$	TS2	$\Delta E^{\text{INT-TC}}$	INT	$\Delta E^{\text{INT-CF}}$	TS1	CF
CTC $\leftrightarrow$ INT $\rightarrow$ CF, $\tau(\text{CTC}) = 17.5$ min in cyclohexane at 21 °C							
CTC <sub>a</sub>							
	0.626 eV 3.51 D	+0.380	1.005 4.02	+0.161	0.844 1.25	+0.341	1.185 1.22
CTC <sub>b</sub>							
	0.610 eV 4.11 D	+0.414	1.024 3.62	+0.166	0.858 2.93	+0.364	1.223 2.10
TTC $\leftrightarrow$ INT $\rightarrow$ CF, $\tau(\text{TTC}) = 17.1$ s in cyclohexane at 21 °C							
TTC <sub>c</sub>							
	0.655 eV 3.13 D	+0.415	1.070 2.17	+0.164	0.906 1.79	+0.254	1.160 1.90
TTC <sub>d</sub>							
	0.669 eV 2.17 D	+0.476	1.145 1.76	+0.207	0.938 1.53	+0.203	1.141 1.90

**Table 1.** Energetics of the two-stepwise process of the TC form depopulation (TC  $\leftrightarrow$  INT  $\rightarrow$  CF). Adiabatic  $S_0$ -state energies,  $E^a$  (in eV), and dipole moment,  $\mu_g$  (in Debye), for the relevant minima: TC, INT, CF, and transition states separating these minima: TS1 and TS2, calculated at the MP2/cc-pVDZ theory level.

be classified as a *single-twist* mechanism (rotation around the  $C_{14}=C_1$  bond) or as a *bicycle-pedal* motion (if the concerted rotation about both double bonds takes place). Both mechanisms are visualized in the excited-state potential energy surface spanned over the two double bonds (Fig. 5). The *single-twist* motion can be seen as a motion along the X axes ( $C_{14}=C_1$  rotation) from the green dot representing the initial TC geometry (upper left corner of the contour plot) towards the red dot (TT form, in the upper right corner). This motion meets the excited state  $S_1^{\text{TW}}$  minimum for which  $C_{13}-C_{14}=C_1-C_2$  dihedral angle is usually a little less than  $90^\circ$ , but it should be considered as the active channel in TC  $\rightarrow$  TT photoisomerization. Alternatively, the *bicycle-pedal* motion is followed along the diagonal of the plot—from the TC form (green dot, upper left corner) towards the bottom right corner. This path encounters the  $S_1^{\text{BP}}$  minimum midway through, which may deactivate through  $S_1 \rightarrow S_0$  internal conversion to repopulate eventually the initial TC geometry in the  $S_0$  state. Inspection of the contour plots in Fig. 5 and energetics in Table S2 shows that the relative energies of  $S_1^{\text{TW}}$  are below  $S_1^{\text{BP}}$  thus the photoisomerization TC  $\rightarrow$  TT is expected to be efficient, as observed in the experiment.

According to theoretical calculations, the replacement of the methoxy group in **2** by a methyl substituent has a low impact since its potential energy surface is also tilted towards the  $S_1^{\text{TW}}$  minimum (see Table S3). Consequently, this system should also easily produce the TT form.

## Conclusions

The synthesized compound **2** shows exceptional properties among the members of 3*H*-naphthopyran family. In the photochromic reaction its colored isomers are formed with longer lifetimes in comparison to that of the reference compound **1**. Under UV irradiation a high accumulation of colored forms is observed in a photostationary

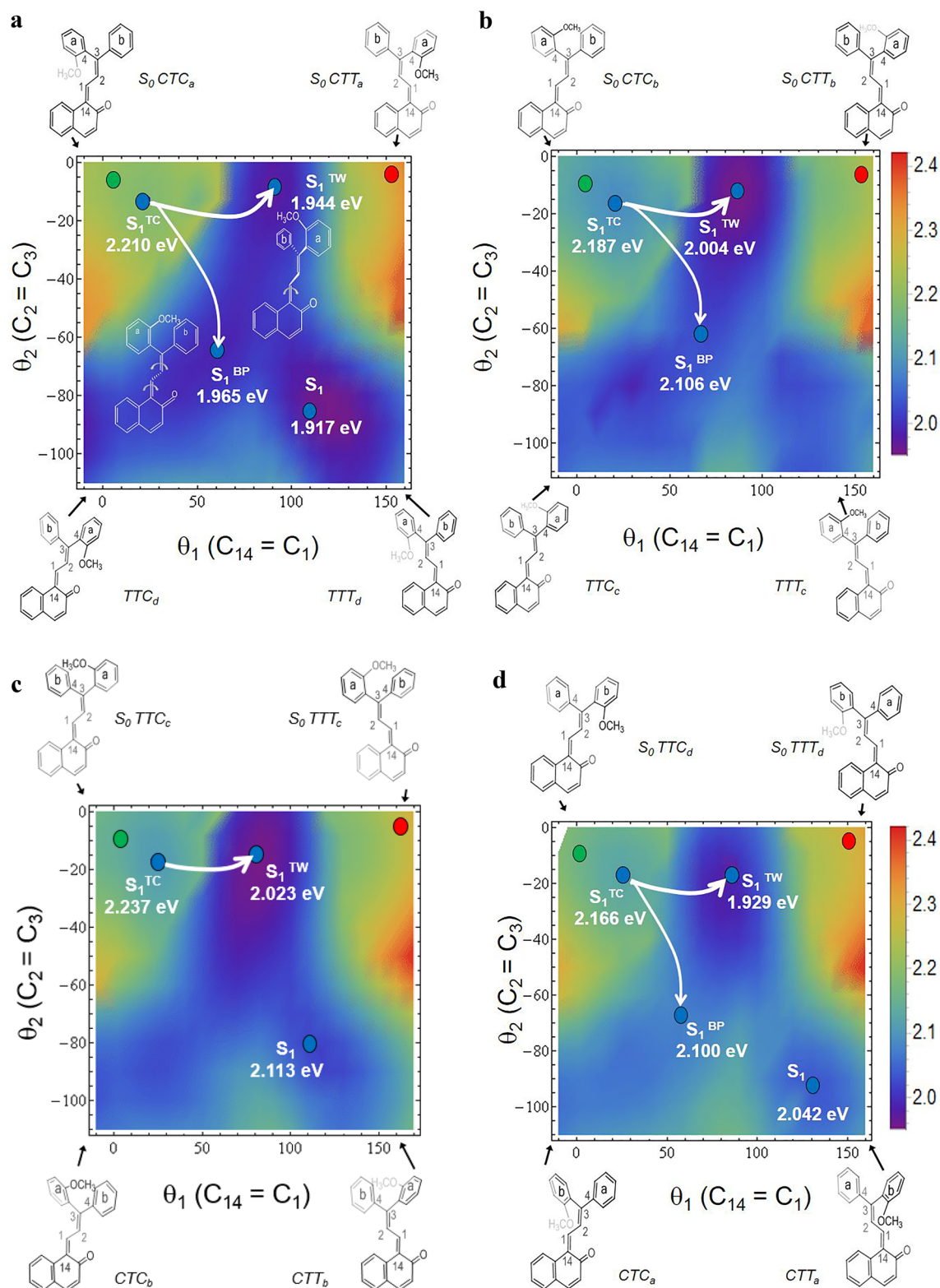


**Figure 5.** Minimum-potential-energy surface of the lowest excited electronic state of the TC-molecule: (a)  $CTC_a$ , (b)  $CTC_b$ , (c)  $TTC_c$  and (d)  $TTC_d$ , plotted as a function of  $\theta_1(C_{14}=C_1)$  and  $\theta_2(C_2=C_3)$  torsional angle coordinates. Green circle represents the Franck–Condon region of the ground-state  $S_0^{TC}$  local minimum and red circle represents the ground-state  $S_0^{TT}$  local minimum. Blue circles represent various types of the excited-state minima:  $S_1^{TC}$ —the minimum initially populated after  $S_0^{TC}$  photoexcitation,  $S_1^{BP}$ —achieved through the *bicycle-pedal* motion, and  $S_1^{TW}$ —reached by *single-twist* motion mechanism. The results were obtained with the aid of the ADC(2)/cc-pVDZ method, for the excited state, and with the MP2/cc-pVDZ, for the ground state.

state. The mechanism of the colored TC form fading process can be analyzed using the energetic landscape of the thermal TC → INT → CF reaction. The determined  $\Delta E^{\text{INT-CF}}$  energy barrier seems to hamper CF repopulation and extends the apparent TC lifetime. Thus, the experimentally determined long lifetime of 17.5 min can be assigned to CTC forms, while the short lifetime of 17.1 s to TTC conformers. The theory suggests also that all TC isomers can undergo photoisomerization by the *single-twist* mechanism around the  $C_{14}=C_1$  angle. The photogenerated TT form is long-lived—the population decay occurs with a single time-constant of 16 h at 21 °C. The proposed photochromic reaction mechanism explains the strong photocolouration effect observed for 2. Theoretical investigations should be considered as an efficient tool for designing new 3H-naphthopyrans derivatives with optimized properties. In other words, the implementation of a promising substituent in 3,3-diphenyl-3H-naphtho[2,1-*b*]pyran skeleton can be first theoretically tested for desired photochromic properties prior to the synthesis efforts.

## Data availability

The datasets generated during the current study are available from the corresponding author on request.

Received: 28 April 2022; Accepted: 10 June 2022

Published online: 24 June 2022

## References

- Crano, J. C., Flood, T., Knowles, D., Kumar, A. & Van Gemert, B. Photochromic compounds: Chemistry and application in ophthalmic lenses. *Pure Appl. Chem.* **68**, 1395–1398. <https://doi.org/10.1351/pac199668071395> (1996).
- Hepworth, J. D. & Heron, B. M. In *Functional Dyes* (ed. Kim, S. H.) 85–135 (Elsevier, 2006).
- Corns, S. N., Partington, S. M. & Towns, A. D. Industrial organic photochromic dyes. *Color. Technol.* **125**, 249–261 (2009).
- Towns, A. In *Applied Photochemistry: When Light Meets Molecules* (eds Giacomo, B. & Serena, S.) 227–279 (Springer International Publishing, 2016).
- Delbaere, S. *et al.* Kinetic and structural studies of the photochromic process of 3H-naphthopyrans by UV and NMR spectroscopy. *J. Chem. Soc. Perkin Trans. 2*, 1153–1157. <https://doi.org/10.1039/A800906F> (1998).
- Ottavi, G., Favaro, G. & Malatesta, V. Spectrokinetic study of 2,2-diphenyl-5,6-benzo(2H) chromene: A thermoreversible and photoreversible photochromic system. *J. Photochem. Photobiol. A* **115**, 123–128 (1998).
- Görner, H. & Chibisov, A. K. Photoprocesses in 2,2-diphenyl-5,6-benzo(2H)chromene. *J. Photochem. Photobiol. A* **149**, 83–89. [https://doi.org/10.1016/S1010-6030\(02\)00002-3](https://doi.org/10.1016/S1010-6030(02)00002-3) (2002).
- Gentili, P. L., Danilov, E., Ortica, F., Rodgers, M. A. J. & Favaro, G. Dynamics of the excited states of chromenes studied by fast and ultrafast spectroscopies. *Photochem. Photobiol. Sci.* **3**, 886–891 (2004).
- Delbaere, S. & Vermeersch, G. NMR characterization of allenyl-naphthol in the photochromic process of 3,3-diphenyl-[3H]-naphtho[2-1, b]pyran. *J. Photochem. Photobiol. A* **159**, 227–232 (2003).
- Herzog, T. T., Ryseck, G., Ploetz, E. & Cordes, T. The photochemical ring opening reaction of chromene as seen by transient absorption and fluorescence spectroscopy. *Photochem. Photobiol. Sci.* **12**, 1202–1209. <https://doi.org/10.1039/C3PP50020A> (2013).
- Brazevic, S., Nizinski, S., Szabla, R., Rode, M. F. & Burdzinski, G. Photochromic reaction in 3H-naphthopyrans studied by vibrational spectroscopy and quantum chemical calculations. *Phys. Chem. Chem. Phys.* **21**, 11861–11870. <https://doi.org/10.1039/C9CP01451A> (2019).
- Brazevic, S., Baranowski, M., Sikorski, M., Rode, M. F. & Burdziński, G. Ultrafast dynamics of the transoid-*cis* isomer formed in photochromic reaction from 3H-naphthopyran. *ChemPhysChem* **21**, 1402–1407. <https://doi.org/10.1002/cphc.202000294> (2020).
- Brazevic, S. *et al.* Control of the photo-isomerization mechanism in 3H-naphthopyrans to prevent formation of unwanted long-lived photoproducts. *Int. J. Mol. Sci.* **21**, 7825. <https://doi.org/10.3390/ijms21217825> (2020).
- Inagaki, Y., Kobayashi, Y., Mutoh, K. & Abe, J. A simple and versatile strategy for rapid color fading and intense coloration of photochromic naphthopyran families. *J. Am. Chem. Soc.* **139**, 13429–13441. <https://doi.org/10.1021/jacs.7b06293> (2017).
- Brazevic, S. *et al.* *Cisoid-cis* intermediate plays a crucial role in decolouration rate in photochromic reaction of 8H-pyranoquinazolines and 3H-naphthopyrans. *Dyes Pigm.* **201**, 110249 (2022).
- Brazevic, S., Sliwa, M., Kobayashi, Y., Abe, J. & Burdzinski, G. Disclosing whole reaction pathways of photochromic 3H-naphthopyrans with fast color fading. *J. Phys. Chem. Lett.* **8**, 909–914. <https://doi.org/10.1021/acs.jpcclett.6b03068> (2017).
- Gabbutt, C. D., Heron, B. M. & Instone, A. C. The synthesis and electronic absorption spectra of 3-phenyl-3(4-pyrrolidino-2-substituted phenyl)-3H-naphtho[2,1-*b*]pyrans: Further exploration of the ortho substituent effect. *Tetrahedron* **62**, 737–745 (2006).
- Alberti, A., Teral, Y., Roubaud, G., Faure, R. & Campredon, M. On the photochromic activity of some diphenyl-3H-naphtho[2,1-*b*]pyran derivatives: synthesis, NMR characterisation and spectrokinetic studies. *Dyes Pigm.* **81**, 85–90 (2009).
- Pardo, R., Zayat, M. & Levy, D. Effect of the chemical environment on the light-induced degradation of a photochromic dye in ormosil thin films. *J. Photochem. Photobiol. A* **198**, 232–236 (2008).
- de Azevedo, O. D. C. C. *et al.* Synthesis and photochromism of novel pyridyl-substituted naphthopyrans. *J. Org. Chem.* **85**, 10772–10796. <https://doi.org/10.1021/acs.joc.0c01296> (2020).
- Zayat, M. & Levy, D. Photochromic naphthopyrans in sol-gel ormosil coatings. *J. Mater. Chem.* **13**, 727–730 (2003).
- Gabbutt, C., Heron, B. M. & Instone, A. C. Control of the fading properties of photochromic 3,3-diaryl-3H-naphtho[2,1-*b*]pyrans. *Heterocycles* **60**, 843–855 (2003).
- Møller, C. & Plesset, M. S. Note on an approximation treatment for many-electron systems. *Phys. Rev* **46**, 618–622. <https://doi.org/10.1103/PhysRev.46.618> (1934).
- Hättig, C. In *Advances in Quantum Chemistry* Vol. 50 (ed. Jensen, H. J. Å.) 37–60 (Academic Press, 2005).
- Schirmer, J. Beyond the random-phase approximation: A new approximation scheme for the polarization propagator. *Phys. Rev. A* **26**, 2395–2416. <https://doi.org/10.1103/PhysRevA.26.2395> (1982).
- Trofimov, A. B. & Schirmer, J. An efficient polarization propagator approach to valence electron excitation spectra. *J. Phys. B: At. Mol. Opt. Phys.* **28**, 2299–2324. <https://doi.org/10.1088/0953-4075/28/12/003> (1995).
- Dunning, T. H. Jr. Gaussian basis sets for use in correlated molecular calculations. I. The atoms boron through neon and hydrogen. *J. Chem. Phys.* **90**, 1007–1023. <https://doi.org/10.1063/1.456153> (1989).
- Christiansen, O., Koch, H. & Jørgensen, P. The second-order approximate coupled cluster singles and doubles model CC2. *Chem. Phys. Lett.* **243**, 409–418. [https://doi.org/10.1016/0009-2614\(95\)00841-Q](https://doi.org/10.1016/0009-2614(95)00841-Q) (1995).
- Hättig, C. & Weigend, F. CC2 excitation energy calculations on large molecules using the resolution of the identity approximation. *J. Chem. Phys.* **113**, 5154–5161. <https://doi.org/10.1063/1.1290013> (2000).
- TURBOMOLE V7.1 2016, a development of University of Karlsruhe and Forschungszentrum Karlsruhe GmbH, 1989–2007, TURBOMOLE GmbH, since 2007; available from <http://www.turbomole.com>.

## Acknowledgements

This work was performed with financial support from the National Science Centre (NCN), Poland, project 2017/27/B/ST4/00320. Calculations were performed at the PL-Grid Infrastructure.

## Author contributions

The following co-authors contributed in particular with; B.G. synthesis, M.R. theoretical calculations, conceptualization, writing original draft and G.B. spectroscopic experiments, formal analysis, supervision, funding acquisition, conceptualization, writing original draft. All authors reviewed the manuscript.

## Competing interests

The authors declare no competing interests.

## Additional information

**Supplementary Information** The online version contains supplementary material available at <https://doi.org/10.1038/s41598-022-14679-9>.

**Correspondence** and requests for materials should be addressed to M.F.R. or G.B.

**Reprints and permissions information** is available at [www.nature.com/reprints](http://www.nature.com/reprints).

**Publisher's note** Springer Nature remains neutral with regard to jurisdictional claims in published maps and institutional affiliations.



**Open Access** This article is licensed under a Creative Commons Attribution 4.0 International License, which permits use, sharing, adaptation, distribution and reproduction in any medium or format, as long as you give appropriate credit to the original author(s) and the source, provide a link to the Creative Commons licence, and indicate if changes were made. The images or other third party material in this article are included in the article's Creative Commons licence, unless indicated otherwise in a credit line to the material. If material is not included in the article's Creative Commons licence and your intended use is not permitted by statutory regulation or exceeds the permitted use, you will need to obtain permission directly from the copyright holder. To view a copy of this licence, visit <http://creativecommons.org/licenses/by/4.0/>.

© The Author(s) 2022